Catalysis Letters 37 (1996) 187–191

Studies on SO_4^{2-} promoted mixed oxide superacids

Changxi Miao, Weiming Hua, Jianmin Chen and Zi Gao [1]

Department of Chemistry, Fudan University, Shanghai 200433, PR China

Received 7 August 1995; accepted 21 November 1995

Sulfated binary and trinary oxide solid superacids were prepared and characterized. The incorporation of Cr, Fe, Mn and V into sulfated zirconia increases its superacidity and catalytic activity for *n*-butane isomerization at 35°C significantly. The catalytic activity of sulfated oxides of Cr–Zr, Fe–Cr–Zr and Fe–V–Zr is 2–3 times greater than that of the well-known sulfated Fe–Mn–Zr oxide. A negative effect was observed in the cases of sulfated Mn–Zr, Sn–Zr, W–Zr and Mo–Zr oxides. The origin of the enhancement in superacidity and activity is discussed in the light of experimental results obtained by XRD, IR and chemical analysis.

Keywords: solid superacids; sulfated binary and trinary oxides; butane isomerization; characterization

1. Introduction

A considerable number of reports dealing with SO_4^{2-} promoted metal oxide solid superacids have appeared recently [1–5]. These superacids are known to have acid strength higher than that of 100% H_2SO_4, and their potential for selective hydrocarbon isomerization has aroused new enthusiasm for the study of the preparation, characterization and catalytic reactivity of this type of catalysts. A new solid superacid, sulfated trinary oxide containing Fe, Mn and Zr, has recently been developed by Hsu et al. [6], and has shown higher superacidity than SO_4^{2-}/ZrO_2. This new catalyst has been reported to be able to isomerize *n*-butane at ambient temperature with a rate three orders of magnitude greater than SO_4^{2-}/ZrO_2. It is inspiring that the incorporation of transition metals may increase the superacidity and catalytic activity of sulfated zirconia, although the nature of such an enhancement is far from clear. In this study, a wide variety of SO_4^{2-} promoted binary and trinary oxide superacids has been investigated for the purpose of searching other more active new solid superacid systems and finding out some generalizations for the development of this type of superacidic catalytic materials.

2. Experimental

Mixed oxides containing Zr and some other metals (such as Fe, Co, Ni, Cr, Ti, Al, Sn and Mn) were prepared by the co-precipitation method. Appropriate amounts of zirconium oxychloride and metal nitrates were dissolved to make mixed solutions. Aqueous ammonia was added for hydrolysis. The precipitate was filtered, and then followed by immersing in a 0.5 mol/ℓ H_2SO_4 aqueous solution for 30 min. The sulfated sample was then dried at 110°C and calcined in dry air at 650°C for 3 h. The other metals (such as V, Mo and W) were incorporated by the incipient wetness method. An appropriate amount of ammonium metavanadate, ammonium molybdate or ammonium metatungstate was dissolved in water. The predried and uncalcined sulfated zirconia was treated with the above solutions, and then dried at 110°C and calcined in dry air at 650°C for 3 h.

X-ray powder diffraction measurements were performed on a Rigaku D/MAX-IIA instrument with monochromatic Cu Kα radiation, scan speed 16°/min and scan range 5–70°. Infrared spectra of the samples were recorded on a Perkin-Elmer 983 G infrared spectrometer. The samples were pressed in the form of thin wafers with the density of 4.5–6.5 mg/cm^2, and placed in a quartz sample cell with NaCl windows. The BET surface areas of the samples were measured on a Micromeritics ASAP 2010 system under liquid N_2 temperature using N_2 as the adsorbent. Chemical method was used for the detection of sulfate content in the samples [3]. Dehydrated Na_2CO_3 and ZnO were utilized as the fusing agents, and the sulfate was turned into $BaSO_4$ and determined by gravimetric method.

n-butane isomerization reaction was carried out at 35°C and 6.5×10^4 Pa in a closed recirculating reactor. The catalyst loading was 0.5 g. The amount of *n*-butane injected for each test was 5 ml of gas (20°C, 1×10^5 Pa). The reaction products were sampled and analyzed by using a gas chromatograph equipped with FID.

3. Results and discussion

Most of the SO_4^{2-} promoted binary and trinary oxide solid superacids prepared in the present paper were

[1] To whom correspondence should be addressed.

© J.C. Baltzer AG, Science Publishers

colored samples. Their acid strength cannot be detected by the conventional Hammett indicator method. It has been reported previously that the activities of the catalysts for *n*-butane isomerization at ambient temperature are dependent on their superacidity, and the isomerization of butane on the catalysts obeys the rate law of first-order reversible reaction after a short induction period of 0.5–3.0 h depending on the activity of the catalysts [7]. In table 1, the forward rate constants k_1 of the *n*-butane isomerization reaction at 35°C measured over different catalysts were compared. Among the sulfated binary oxides, the addition of Cr increases the catalytic activity of the sulfated oxide most evidently. The *n*-butane isomerization activity of SO_4^{2-}/1.5% Cr/ZrO_2 is 6–7 times higher than that of SO_4^{2-}/ZrO_2. The addition of either V, Ti, Al, Fe, Ni or Co enhances the catalytic activity only slightly, while the addition of Mo, W, Mn or Sn diminishes the catalytic activity. Comparing the data of the sulfated trinary oxides, it is clear that the combination of Mn or V and Cr cannot further improve the catalytic activity of the Cr–Zr binary oxide system, but the addition of a third metal component to the Fe–Zr binary oxide system may increase its catalytic activity remarkably. SO_4^{2-}/1.5% Fe/0.5% V/ZrO_2 and SO_4^{2-}/1.5% Fe/0.5% Cr/ZrO_2 are 8–9 times more active than SO_4^{2-}/ZrO_2 and 2–3 times more active than the famous SO_4^{2-}/1.5% Fe/0.5% Mn/ZrO_2. It should be noted that the activity difference between SO_4^{2-}/1.5% Fe/0.5% Mn/ZrO_2 and SO_4^{2-}/ZrO_2 in our hands is not as eminent as in the literature [8,9]. This is probably caused by the differences in the ways of activity test and catalyst preparation. In our work the samples were tested under the same temperature in a closed recirculating reactor with almost the same conversion level. At least 8 to10 data points were used for the fitting of the rate constants k_1, and in the most cases the correlation coefficients of fitting were $\geqslant 0.99$. However, Hsu et al. measured the activity of the catalysts in a flow-type reactor with a large difference in reaction temperature and conversion level, and only 2 or 3 data points were used for the extrapolation of the reaction rate. Besides, the activity of the SO_4^{2-}/ZrO2 catalyst in Hsu's work is rather low. The conversion of *n*-butane on their SO_4^{2-}/ZrO_2 at 100–140°C reported is < 2.2%, whereas the conversion of *n*-butane on our SO_4^{2-}/ZrO_2 catalyst is up to 4.5–14.7% at 100°C and a space velocity of 1.0–0.3 h^{-1}. On the other hand, the results in table 1 show that the incorporation of a second and a third metal component may affect the superacidity and the catalytic activity of the superacid systems either positively or negatively depending on the nature of the metal components.

Zirconia may exist in two crystal phases after calcination below 800°C: a metastable tetragonal phase and a thermodynamically favored monoclinic phase [10]. It has been reported that sulfation retards the crystallization of hydrous zirconium oxide and stabilizes the tetragonal phase [2]. Some of the papers [11,12] stated that the transformation from the metastable tetragonal phase to the monoclinic phase is related to the deterioration of the superacidity of the sample. XRD patterns of the sulfated binary and trinary oxides after calcination at 650°C were recorded. The characteristic peaks of the

Table 1
n-butane isomerization activity at 35°C

Sample	Reaction time (h)	Conversion (%)	Isomerization selectivity (%)	$k_1 \times 10^3$ (h^{-1})
SO_4^{2-}/ZrO_2	20	35.0	98.1	40.1
SO_4^{2-}/0.5% Cr/ZrO_2	20	43.4	100	55.2
SO_4^{2-}/1.5% Cr/ZrO_2	4	45.8	100	290.6
SO_4^{2-}/3.0% Cr/ZrO_2	4	41.2	100	270.6
SO_4^{2-}/6.0% Cr/ZrO_2	20	36.8	96.2	40.6
SO_4^{2-}/1.5% V/ZrO_2	20	39.9	100	44.7
SO_4^{2-}/1.5% Ti/ZrO_2	20	39.5	99.5	43.6
SO_4^{2-}/1.5% Al/ZrO_2	20	39.8	97.4	42.8
SO_4^{2-}/1.5% Fe/ZrO_2	20	38.8	97.5	42.7
SO_4^{2-}/1.5% Ni/ZrO_2	20	38.7	97.6	41.1
SO_4^{2-}/1.5% Co/ZrO_2	20	35.1	98.7	40.7
SO_4^{2-}/1.5% Mn/ZrO_2	20	24.4	98.2	19.2
SO_4^{2-}/1.5% Sn/ZrO_2	20	22.7	98.0	11.7
SO_4^{2-}/1.5% Mo/ZrO_2	20	11.4	100	8.3
SO_4^{2-}/1.5% W/ZrO_2	20	4.8	100	3.0
SO_4^{2-}/1.5% Cr/0.5% Mn/ZrO_2	6	31.3	100	110.8
SO_4^{2-}/1.5% Cr/0.5% V/ZrO_2	6	40.2	100	152.2
SO_4^{2-}/1.5% Fe/0.5% Mn/ZrO_2	6	39.8	95.0	134.8
SO_4^{2-}/1.5% Fe/0.5% V/ZrO_2	4	51.4	99.0	350.5
SO_4^{2-}/1.5% Fe/0.5% Cr/ZrO_2	4	47.7	100	334.5
SO_4^{2-}/1.5% Fe/0.5% Bi/ZrO_2	6	29.4	95.0	95.2
SO_4^{2-}/1.5% Fe/0.5% Mo/ZrO_2	6	25.7	97.9	94.1
SO_4^{2-}/1.5% Fe/0.5% W/ZrO_2	6	35.3	95.6	113.7

metal oxides except ZrO_2 are not observed, implying that the metal oxides are present in the form of oxide solid solutions or highly dispersed on the surface of ZrO_2. Besides, the addition of metal components results in an increase in the crystallization temperature of ZrO_2 at least by 50°C. Figs. 1 and 2 depict the XRD patterns of the samples calcined at 550 and 650°C, respectively. In sulfated zirconia ZrO_2 crystallizes almost completely at 550°C, and both tetragonal and monoclinic phases are present. In the binary and trinary oxide systems the crystallization process completes at higher temperatures and the occurrence of tetragonal-to-monoclinic transformation is dependent on the nature of the metals. The incorporation of Fe, Cr, Fe–Mn, Cr–Mn, Fe–V and Cr–V retards the phase transformation, while the incorporation of W and Mo does not show such an effect. XRD patterns of a series of samples containing Cr from 0.5 to 6.0 wt% are shown in fig. 3. It is surprising that the transformation of tetragonal to monoclinic phase is also dependent on the content of Cr in the binary oxides. When the Cr content is in the range of 1.0–3.0 wt%, the phase transformation is inhibited. Outside this range both tetragonal and monoclinic phases are present in the samples after calcination at 650°C. All our experimental results showed that samples exhibiting higher stability of the tetragonal phase have higher superacidity and better catalytic activity for *n*-butane isomerization. This is probably because the readiness for the tetragonal to monoclinic transformation of ZrO_2 reflects the chemical

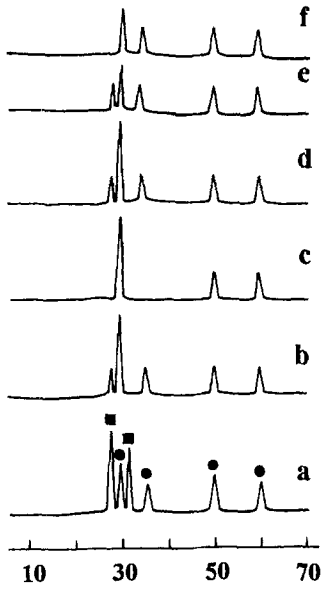

Fig. 1. XRD patterns of various samples calcined at 550°C. (a) ZrO_2; (b) SO_4^{2-}/ZrO_2; (c) SO_4^{2-}/1.5% Fe/ZrO_2, SO_4^{2-}/1.5% Cr/ZrO_2; (d) SO_4^{2-}/1.5% W/ZrO_2; (e) SO_4^{2-}/1.5% Mo/ZrO_2; (f) SO_4^{2-}/1.5% Fe/0.5% Mn/ZrO_2, SO_4^{2-}/1.5% Cr/0.5% Mn/ZrO_2, SO_4^{2-}/1.5% Cr/0.5% V/ZrO_2, SO_4^{2-}/1.5% Fe/0.5% Cr/ZrO_2, SO_4^{2-}/1.5% Fe/0.5% V/ZrO_2. (●) Tetragonal phase; (■) monoclinic phase.

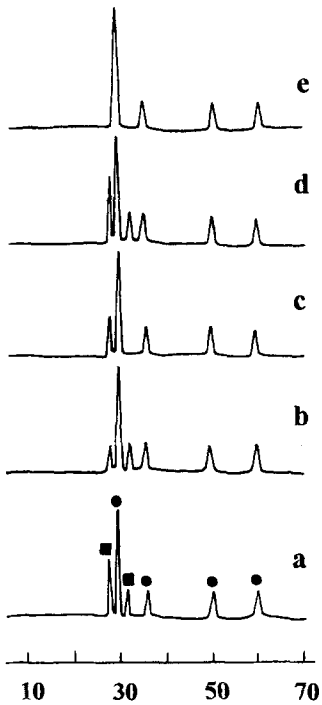

Fig. 2. XRD patterns of various samples calcined at 650°C. (a) SO_4^{2-}/ZrO_2; (b) SO_4^{2-}/1.5% Fe/ZrO_2; (c) SO_4^{2-}/1.5% W/ZrO_2; (d) SO_4^{2-}/1.5% Mo/ZrO_2; (e) SO_4^{2-}/1.5% Cr/ZrO_2, SO_4^{2-}/1.5% Fe/0.5% Mn/ZrO_2, SO_4^{2-}/1.5% Cr/0.5% Mn/ZrO_2, SO_4^{2-}/1.5% Cr/0.5% V/ZrO_2, SO_4^{2-}/1.5% Fe/0.5% Cr/ZrO_2, SO_4^{2-}/1.5% Fe/0.5% V/ZrO_2. (●) Tetragonal phase; (■) monoclinic phase.

state of the sample surface. Factors, such as the formation of oxide solid solutions and enhancement of the quantity and bonding of the sulfate groups on the oxide surface, will retard the phase transformation of ZrO_2, whereas they may cause an increase in superacidity and catalytic activity at the same time.

The specific surface areas and sulfur contents of some typical binary and trinary oxide solid superacid samples after calcination at 650°C for 3 h are listed in table 2. The surface areas of the binary and trinary oxide superacids do not change very much. The differences observed between them and that of SO_4^{2-}/ZrO_2 are in the range of ±30%, which are obviously much smaller than the activity differences. As compared with SO_4^{2-}/ZrO_2, the sulfur contents of the binary and trinary oxide superacids are increased from 0–30%. It seems that there is some correlation between the sulfate concentration and the catalytic activity. The more active catalysts have higher sulfate concentrations, but a direct proportion of the catalytic activity to the sulfate concentration is not found because the result from chemical analysis represents the total sulfate concentration on the oxide surface but not the effective catalytic sites.

Infrared spectra of sulfated zirconia solid superacids after evacuation at 300°C for 3 h display four adsorption bands at 1390, 1190, 1020 and 930 cm^{-1} in the SO

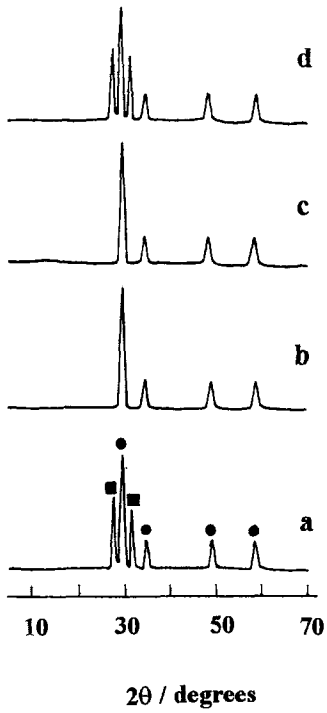

Fig. 3. XRD patterns of Cr-incorporated samples calcined at 650°C. (a) SO_4^{2-}/0.5% Cr/ZrO_2; (b) SO_4^{2-}/1.5% Cr/ZrO_2; (c) SO_4^{2-}/3.0% Cr/ZrO_2; (d) SO_4^{2-}/6.0% Cr/ZrO_2. (●) Tetragonal phase; (■) monoclinic phase.

stretching frequency region. The former two and the latter two bands are assigned to the asymmetric and symmetric stretching frequencies of the O=S=O and O–S–O groups, respectively [13]. The 1390 cm^{-1} band representing the asymmetric stretching frequency of S=O is often regarded as the characteristic band of SO_4^{2-} promoted superacids. When water is adsorbed on the surface sulfur complex at ambient temperature, a red shift of the IR band indicating a strong interaction between the adsorbed molecule and the surface sulfur complex is observed. This frequency shift corresponding to a decrease in the bond order of SO covalent double bond and an increase in the partial charge on oxygen atom is associated with the acid strength of the sample [14]. The electron structures of the surface sulfur complex before and after water adsorption may be illustrated as follows:

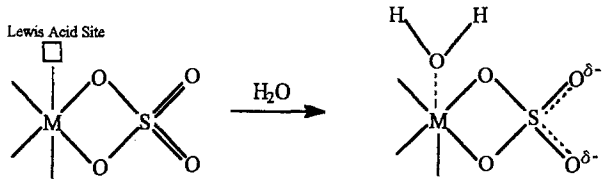

The IR stretching frequency and the bond order and partial charge on oxygen of the SO bond calculated according to equations proposed by Gillespie et al. [15] and Jin et al. [13] for the binary and trinary oxide solid superacids before and after water adsorption are listed in table 3. The increases in IR frequency shift and partial charge on oxygen of the samples are in the order of SO_4^{2-}/1.5% Fe/0.5% V/ZrO_2 > SO_4^{2-}/1.5% Fe/0.5% Cr/ZrO_2 > SO_4^{2-}/1.5% Cr/ZrO_2 > SO_4^{2-}/1.5% Fe/0.5% Mn/ZrO_2 > SO_4^{2-}/1.5% Fe/ZrO_2 > SO_4^{2-}/ZrO_2 > SO_4^{2-}/1.5% W/ZrO_2, which is exactly the same as the order of their superacidity and *n*-butane isomerization activity. This is consistent with our previous results of reaction and IR spectroscopic studies [4,14], which show that the active sites for isomerization of *n*-alkane on superacid catalysts are the superacidic Brønsted acid sites produced via the adsorption of water on the strong Lewis acid sites. Thus, we may suggest that the incorporation of a second metal component (Fe or Cr) and a third metal component (V, Cr or Mn) increases the acid strength and hence the *n*-butane isomerization activity of sulfated zirconia via electronic interactions, while the introduction of some other metal (W, Mo) may produce a negative effect. Introducing metal cations, such as Fe^{3+}, Cr^{3+}, Mn^{4+} and V^{5+}, into the ZrO_2 crystal lattice, the following complex structures may be formed in some local areas on the surface of the samples:

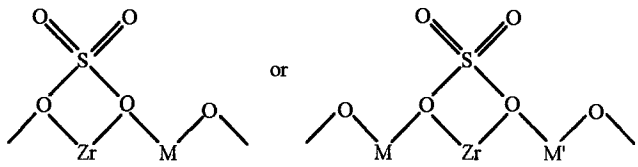

M and M′ = Fe^{3+}, Cr^{3+}, Mn^{4+}, V^{5+}

Table 2
Surface area and sulfur content of various samples

Sample	Surface area (m^2/g)	SO_3 content (wt%)	$k_1 \times 10^3$ (h^{-1})
SO_4^{2-}/ZrO_2	129.3	3.30	40.1
SO_4^{2-}/1.5% Cr/ZrO_2	135.3	3.85	290.6
SO_4^{2-}/1.5% Fe/ZrO_2	129.3	3.47	42.7
SO_4^{2-}/1.5% W/ZrO_2	101.3	3.37	3.0
SO_4^{2-}/1.5% Cr/0.5% Mn/ZrO_2	167.6	4.31	110.8
SO_4^{2-}/1.5% Cr/0.5% V/ZrO_2	114.4	4.15	152.2
SO_4^{2-}/1.5% Fe/0.5% Mn/ZrO_2	104.9	4.22	134.8
SO_4^{2-}/1.5% Fe/0.5% V/ZrO_2	104.0	4.07	350.5

Table 3
Stretching frequency, bond order and partial charge on oxygen of S=O before and after water adsorption

Sample	SO asymmetric stretching frequency (cm^{-1})			Bond order		Partial charge on oxygen		$k_1 \times 10^3$ (h^{-1})
	before water adsorption	after water adsorption	frequency shift	before water adsorption	after water adsorption	before water adsorption	after water adsorption	
SO_4^{2-}/ZrO_2	1392	1352	40	1.87	1.80	−0.13	−0.20	40.1
SO_4^{2-}/1.5%Cr/ZrO_2	1384	1330	54	1.85	1.77	−0.15	−0.23	290.6
SO_4^{2-}/1.5%Fe/ZrO_2	1391	1348	43	1.86	1.80	−0.14	−0.21	42.7
SO_4^{2-}/1.5%W/ZrO_2	1394	1368	26	1.87	1.83	−0.13	−0.17	3.0
SO_4^{2-}/1.5%Fe/0.5%Mn/ZrO_2	1385	1336	49	1.85	1.78	−0.15	−0.22	134.8
SO_4^{2-}/1.5%Fe/0.5%Cr/ZrO_2	1380	1315	65	1.85	1.74	−0.15	−0.26	334.5
SO_4^{2-}/1.5%Fe/0.5%V/ZrO_2	1375	1309	66	1.84	1.74	−0.16	−0.27	350.5

According to the principle of electronegativity equalization proposed by Sanderson [16], the electronegativity S_{int} of the above complex structure and the partial charge δ_{Zr} on Zr^{4+} can be written as

$$S_{int} = [S_M^x S_{M'}^y S_{Zr} S_S S_O^z]^{1/2+x+y+z}, \quad (1)$$

$$\delta_{Zr} = (S_{int} - S_{Zr})/2.08 S_{Zr}^{1/2}, \quad (2)$$

where S_M, $S_{M'}$, S_{Zr}, S_S and S_O are the electronegativities of M, M′, Zr, S and O and x, y, z are the numbers of M, M′ and O in the neighborhood of Zr^{4+}. Among all the metal cations, the electronegativity of Zr^{4+} is very small. The electronegativities of Fe^{3+}, Cr^{3+}, Mn^{4+} and V^{5+} are all relatively larger than that of Zr^{4+}. The electronegativity of the surface complex S_{int} is increased and δ_{Zr} becomes more positive when these metal cations are introduced into the complex, hence the acid strength of the superacidic Lewis acid site is increased. This may qualitatively explain the acidity and activity enhancement observed in many of the sulfated binary and trinary oxide superacid systems.

References

[1] K. Arata, Adv. Catal. 37 (1990) 165.
[2] B.H. Davis, R.A. Keogh and R. Srinivasan, Catal. Today 20 (1994) 219.
[3] Z. Gao, J.M. Chen and Y. Tang, Chem. J. Chinese Univ. 13 (1992) 1498.
[4] Z. Gao, J.M. Chen and Y. Tang, Acta Chim. Sinica 52 (1994) 36.
[5] Z. Gao, J.M. Chen and Y.N. Yao, Chem. J. Chinese Univ. 16 (1995) 111.
[6] E.J. Hollstein, J.T. Wei and C.Y. Hsu, US Patents 4,918,041, 4,956,519 (1990).
[7] Z. Gao, J.M. Chen, W.M. Hua and Y. Tang, *Acid–Base Catalysis II* (Kodansha, Tokyo, 1994) p. 507.
[8] C.Y. Hsu, C.R. Heimbuch, C.T. Armes and B.C. Gates, J. Chem. Soc. Chem. Commun. (1992) 1645.
[9] A. Jatia, C. Chang, J.D. MacLeod, T. Okubo and M.E. David, Catal. Lett. 25 (1994) 21.
[10] A.H. Heuer and M. Rühle, in: *Advances in Ceramics*, Vol. 12, eds. N.C. Claussen, M. Rühle and A.H. Heuer (Am. Ceram. Soc., Columbus, 1984) pp. 1–13.
[11] T. Yamaguchi and K. Tanabe, Mater. Chem. Phys. 16 (1986) 67.
[12] F.R. Chen, G. Coudurier, J.F. Joly and J.C. Vedrine, J. Catal. 143 (1993) 616.
[13] T. Jin, T. Yamaguchi and K. Tanabe, J. Phys. Chem. 90 (1986) 4794.
[14] Z. Gao, J.M. Chen and Y. Tang, Chem.J. Chinese Univ. 14 (1993) 658.
[15] R.J. Gillespie and E.A. Robinson, Can. J. Chem. 41 (1963) 2074.
[16] R.T. Sanderson, *Chemical Bonds and Bond Energy* (Academic Press, New York, 1976) p. 75.